Journal of Molecular Structure 1239 (2021) 130539

Contents lists available at ScienceDirect

Journal of Molecular Structure

journal homepage: www.elsevier.com/locate/molstr

Computer-aided anticancer drug design: *In vitro* and *in silico* studies of new iminocoumarin derivative

Serda Kecel-Gunduz[a], Yasemin Budama-Kilinc[b,*], Bahar Gok[c], Bilge Bicak[a], Gizem Akman[d], Busra Arvas[e], Feray Aydogan[e], Cigdem Yolacan[e]

[a] *Istanbul University, Faculty of Science, Physics Department, Istanbul 34134, Turkey*
[b] *Yildiz Technical University, Faculty of Chemical and Metallurgical Engineering, Department of Bioengineering, Istanbul 34220, Turkey*
[c] *Yıldız Technical University, Graduate School of Natural and Applied Science, Department of Bioengineering, Istanbul 34220, Turkey*
[d] *Department of Biology, Science Faculty, Istanbul University, Istanbul 34134, Turkey*
[e] *Department of Chemistry, Yildiz Technical University, Davutpasa Campus, Istanbul 34220, Turkey*

ARTICLE INFO

Article history:
Received 5 February 2021
Revised 8 April 2021
Accepted 17 April 2021
Available online 27 April 2021

Keywords:
Iminocoumarin derivative
Anticancer drug
Mutagenity
Molecular docking
Cell culture
Cytotoxicity

ABSTRACT

In this study, the aim was computer-aided design of a new anti-cancer drug molecule. For this purpose, 7-hydroxy-8-(((1-hydroxy-3-phenylpropan-2-yl)imino)methyl)-4-(trifluoromethyl)-2*H*-chromen-2-one (D3) was synthesized by the condensation reaction. Its characterization studies were performed by NMR, FTIR, MS and UV spectral data. Anti-cancer activity of D3 was examined on MCF-7, HeLa and Mat-Lylu cell lines, and it was found that D3 showed cytotoxic activity in all cell lines. Mutagenity of D3 was determined by Ames/Salmonella assay, and it was found that it had no mutagenic effect on *S. typhimurium* TA98 and TA100 strains. Antioxidant activity of D3 was also revealed. Besides, the interaction of D3 with DNA was investigated by the UV titration method. Experimental results showed D3 binds to DNA by intercalation or groove linking. Moreover, molecular docking approach was used to elucidate the atomic level interaction between the synthesized compound and DNA; thus, the atomic level behavior of the compound in the binding site of DNA was characterized and its binding properties were determined. In addition, the physicochemical and pharmacokinetic properties of the synthesized compound were performed using ADMET and frontier orbital analyses. In conclusion, according to both *in vitro* and *in silico* findings, it can be suggested that D3 may be used as a new anti-cancer drug for breast, cervical and prostate cancers.

1. Introduction

Coumarins are an important class of oxygen-containing heterocyclic compounds with benzopyrone (1,2-benzopyrone or 2*H*-1-benzopyran-2-one) skeleton. Natural and synthetic coumarin derivatives attract the interest of researchers because of their wide biological activity. Some of the derivatives as warfarin have already been used as a drug. Many of the coumarin derivatives have been proven to have important biological activities such as antitumor, antibacterial, antifungal, anticoagulant, antioxidant, antiviral etc. activities. Coumarin skeleton can easily be functionalized from a different position to design new derivatives with promising biological activities [1–11].

Up to now, various drugs for cancer treatment have been developed, but due to their serious side effects, medicinal and pharmaceutical chemists work hard to develop effective anticancer drugs with promising bioactivity, important therapeutic effect [12] and limited toxicity [13]. Coumarin derivatives have been extensively investigated as antitumor agents and it has been shown that they can act on various tumor cells by different mechanisms [14,15]. This derivatives, which are frequently found in nature, exhibit a potential anticancer activity against a wide variety of cancer cell lines as they can easily interact with a wide variety of enzymes and receptors such as kinase, telomerase, aromatase, sulfatase, monocarboxylate transporters and carbonic anhydrase [16]. Also, coumarin derivatives have shown the cytotoxic effect on various cancer cells such as lung, ovarian, breast, prostate, colon, gastric cancer and leukaemia [17–23].Antioxidant compounds neutralize free radicals and reduce the risk for chronic diseases by minimizing the oxidative damage. Hydroxycoumarins are phenolic compounds that act as free radical scavengers since their hy-

* Corresponding author at: Faculty of Chemical and Metallurgical Engineering, Department of Bioengineering, Yildiz Technical University, Istanbul 34220, Turkey.
E-mail address: yaseminbudama@gmail.com (Y. Budama-Kilinc).

https://doi.org/10.1016/j.molstruc.2021.130539
0022-2860/

droxyl groups are potent electron/hydrogen donors to free radicals. Many coumarin derivatives have special abilities to scavenge reactive oxygen species [24–33].

Iminocoumarin is a subclass of coumarin family. The imino group, including Schiff bases compound, is important for several biological applications [34–39]. It is examined that Schiff bases is related with antimicrobial, antiviral and anticancer activity. Thus, iminocoumarins are also important structures that stand out in biological and medical applications and have anticancer and antimicrobial properties [40–43]. Imino coumarin, have also anticancer properties [34] on different human cancer cell lines such as coumarin derivatives [44–46] on prostate [8,47,48], on breast [49], and on cervical cancer cell lines [50].

Encouraging improvements in biological activities showed by coumarins direct the researcher's attention to design and synthesis of new more effective derivatives. But still there is need to develop effective anticancer drugs.

In developing a new drug, it is evaluated three basic criteria: efficacy, quality and pharmacological safety. Regulatory bodies such as the Food and Drug Administration (FDA), the European Medicines Agency (EMA) and the National Health Surveillance Agency (Anvisa) state that preclinical trials should be the starting point for a new drug development process [51–53]. DNA is the target in the development of new anticancer drugs. In this context, understanding the interactions of small molecules with DNA is important for developing new and effective drugs for clinical applications. In addition, the Ames/Salmonella assay is a routine part of preclinical trials in determining the safety of a new drugs [54].

Uncovering the DNA binding properties of coumarin compounds, which have antitumor, antioxidant, antiviral, antibacterial, antifungal properties, has an important place in the development of new therapeutic reagents. In this study, spectroscopic (UV / VIS) and in silico methods (molecular docking) were used to determine the relationship of the coumarin compound with the property of being a potential anticancer drug, and its interaction mechanism was investigated at the atomic level.

To investigate the mutagenic effects and antioxidant activity of D3, Ames/Salmonella assay and diphenyl-2-picrylhydrazyl (DPPH) radical scavenger test were performed. The cytotoxic activity of D3 was also studied via MTT assay using human breast cancer (MCF-7), human epithelial cervical cancer (HeLa) and rat prostate cancer (MAT-Lylu).

2. Materials and methods

2.1. Materials and equipments

Reagent quality solvents were used without further purification. Column chromatography was conducted on silica gel 60 (40–63 μM) (Merck). TLC was carried out on aluminum sheets precoated with silica gel 60F_{254} (Merck). IR spectra were determined on a Thermo Scientific NICOLET IS10 spectrometer. NMR spectra were recorded on Bruker Avance III 500 MHz spectrometer. Chemical shifts, δ are reported in ppm with TMS as internal standard and the solvents are $CDCl_3$. LC-MS (QTOF) spectra were obtained on Agilent G6530B model TOF/Q-TOF Mass Spectrometer. The synthesis of compounds **1** and **2** were carried out according to the literature procedure [55,56].

Calf thymus DNA (CT-DNA), 1,1-Diphenyl-2-picril-hydrazine (DPPH), ethanol, magnesium sulfate heptahydrate ($MgSO_4.7H_2O$), citric acid monohydrate ($C_6H_8O_7.H_2O$), potassium phosphate (K_2HPO_4), sodium dihydrogen phosphate monohydrate ($NaH_2PO_4.H_2O$), sodium hydroxide (NaOH), sodium chloride (NaCl), disodium hydrogen phosphate dihydrate ($Na_2HPO_4.2H_2O$), potassium chloride (KCl) agar (Difco), nutrient broth (Oxoid no: 2) L-histidine, D-biotin, sodium ammonium phosphate tetrahydrate ($NaHNH_4(PO_4.4H_2O)$) and 4-nitro-o-phenylenediamine (NPD) were purchased from Sigma Aldrich. Sodium azide (SA, NaN_3), dimethyl sulfoxide (DMSO), tris base, ethylenediamintetraacetic acid (EDTA), hydrochloric acid (HCl), sodium hydroxide (NaOH) were purchased from Merck Millipore. DMEM, MTT and dexometasone were acquired from Sigma–Aldrich. Penicillin and streptomycin were purchased from I.E. Ulagay. DMSO, which is used for MTT assay was obtained from Merck. RPMI-1640 Medium, FBS, Trypsin, PBS, L-glutamine were obtained from Gibco. Absorbances were measured with BioTek, ELx800 Microplate Reader.

2.2. Methods

2.2.1. Synthesis of 7-hydroxy-8-(((1-hydroxy-3-phenylpropan-2-yl)imino)methyl)-4-(trifluoromethyl)-2H-chromen-2-one (D3)

2-Amino-3-phenyl-1-propanol (1 mmol) and 8-formyl-7-hydroxy-4-(trifluoromethyl)coumarin (**2**, 1 mmol) were dissolved in absolute ethanol. The mixture was refluxed under inert atmosphere for 4 h. The reaction was monitored by TLC. Then alcohol was evaporated, and the crude product was purified by column chromatography on silica gel (ethyl acetate-hexane 1:1). Yellow solid, m.p. 193.1–196.2 °C, yield 92%. ^{1}H NMR (500 MHz, $CDCl_3$, δ): 2.92 (dd, 1H, J = 13.7, 8.5 Hz, CH_2Ph), 3.05 (dd, 1H, J = 13.5, 5.0 Hz, CH_2Ph), 3.72 (dd, 1H, J = 11.5, 8.0 Hz, CH_2OH), 3.78–3.80 (m, 1H, CH), 3.94 (apparent dd, 1H, J = 11.5, 2.5 Hz, CH_2OH), 4.72 (bs, 1H, OH), 6.32 (s, 1H, =CH), 6.50 (d, 1H, J = 9.5 Hz, ArH), 7.15 (d, 2H, J = 6.5 Hz, ArH), 7.21–7.24 (m, 1H, ArH), 7.28–7.32 (m, 3H, ArH), 8.50 (s, 1H, CH=N); ^{13}C NMR (125 MHz, $CDCl_3$, δ): 37.9 (CH_2Ph), 64.4 (CH), 68.9 (OCH_2), 100.7 (C-3), 104.1 (C_{aro}H, C-7), 108.1 (C_{aro}, C-5), 120.0 (C_{aro}H), 122.4 (C_{aro}H), 127.2 (C_{aro}H), 128.9 (C_{aro}H), 129.2 (C_{aro}), 130.1 (C_{aro}), 135.8 (C_{aro}), 141.9 (C_q, J_{CF}=130 Hz, CF_3), 157.0 (C-4), 158.6 (C_{aro} and C–OH), 160.0 (C=N), 176.2 (C=O) ppm. FTIR (ATR): ν = 3551, 3419, 3061, 3028, 2946, 2855, 1723, 1629, 1575, 1496, 1381, 1284 cm^{-1}; LC-MS (ESI-QTOF): m/z [M-H]$^+$ calcd for $C_{20}H_{16}F_3NO_4$, 390.0953; found, 390.0977.

2.2.2. DNA binding assay

DNA binding assay was performed using the UV–vis absorption titration method in Tris-HCl/NaCl buffer (pH 7.2) at room temperature. The purity of the CT-DNA solution in Tris-HCl / NaCl buffer was confirmed as 1.9 ratio which is the ratio of UV absorbance values at 260 and 280 nm wavelengths. This ratio indicates that the CT-DNA is free of protein impurities [57,58]. The experiment was carried out by keeping the D3 concentration (30 µM) constant in the buffer and adding increasing concentrations (0–270 µM) of CT-DNA. The solutions were incubated for 5 min at room temperature, and then spectra were recorded. The percentage ratio of changes in the absorbance intensity of D3 was calculated by the following formula (Eq (1)).

$$\%H = [(A_i - A_s) / (A_i)] \times 100 \quad (1)$$

in this equation, Ai indicates the free absorbance intensity of the compound, and as indicates the absorbance intensity of the compound after adding DNA at the maximum concentration.

The intrinsic binding constant (K_b) used to investigate the binding strength of the D3 molecule to DNA was calculated using Eq. (2). In the formula, ε_A; damping coefficient in the measured concentross, ε_b; damping coefficient after binding of all compounds to DNA and ε_f; damping coefficient of the free compound. In the [DNA]/($\varepsilon_A - \varepsilon_f$) versus [DNA] plot, the ratio of the slope to the point of intersection gives K_b [57].

$$[DNA] / (\varepsilon_A - \varepsilon_f) = [DNA] / (\varepsilon_B - \varepsilon_f) + 1 / K_b(\varepsilon_B - \varepsilon_f) \quad (2)$$

2.2.3. Mutagenity assay

The Ames/Salmonella assay is the most widely used test among bacterial mutation tests to investigate the mutagenic effects of chemicals [59]. The strains of *S. typhimurium*, TA98 and TA100 are widely used in the Ames test, and they are very sensitive in detecting the majority of known bacterial mutagens [60].

TA98 and TA100 mutant strains of *S. typhimurium* were used in our study. The genotypes of test strains (histidine requirement, rfa mutation, uvr B mutation, and pKM101 plasmid) were routinely checked [61]. In the experiment, 100 µL of 1–2 × 10^9 bacteria, 100 µL of D3 in different concentrations (6.25, 12.5, 25 and 50 µg / mL), 500 µL of phosphate buffer (pH=7.4) were added to 2 mL ball agar containing 222 µL of histidine / biotin (0.5 mM) for both *S. typhimurium* strains, and mixed vigorously on a vortex mixer. Then, minimal glucose was poured onto the surface of the agar plate. Negative control plates, (100 µL DMSO + 100 µL bacteria +500 µL buffer) and spontaneous control plates (100 µL bacteria +500 µL buffer) were also prepared. After then, positive control of TA98 (100 µL 4-nitro-o-phenylenediamine +100 µL bacteria +500 µL) and TA100 (100 µL sodium azide + 100 µL bacteria +500 µL buffer) were prepared. After 48 h of incubation at 37 °C, D3 treated plates were compared with negative control plates for mutagenicity. Experiments were carried out in triplicate for each sample.

2.2.4. Antioxidant activity

Antioxidant activity of D3 was determined by diphenyl-2-picrylhydrazyl (DPPH) radical scavenger test. The ability of D3 to scavenge the stable free radical DPPH was measured spectrophotometrically by a continuous decrease in absorbance at 517 nm in the presence of antioxidants [62]. Four different concentrations (6.25, 12.5, 25 and 50 µg / mL) of D3 samples were used similar to the mutagenity assay result. The stock solution of DPPH (25 µg / mL) was prepared in ethanol, and 0.5 ml of this stock solution was added to each sample. After incubation in the dark for 20 min, the absorbance values were read at 517 nm using a UV–vis spectrophotometer. BHT (Butyl Hydroxy Toluene) was used as the standard antioxidant, and percent inhibition of DPPH radical was calculated using Eq (3) [63]. In this equation, A_C indicates absorbance of control, and A_S indicates absorbance of test sample.

$$\%\,\text{Inhibition} = [(A_C - A_S) / A_C] \times 100 \quad (3)$$

2.2.5. HOMO LUMO analysis

For the determination of frontier molecular orbitals required to obtain properties such as chemical stability, ionization potential, electron affinity, chemical hardness of the synthesized compound under different environmental conditions, Gaussian program [64] and time-dependent density functional theory (TD-DFT) [65] approach with B3LYP / 6-311 ++ G (d, p) basis set [66] were used.

2.2.6. Molecular docking and ADME analysis

In this study, the molecular structure of the synthesized D3, as a ligand, was drawn and optimized with the DFT/B3LYP/6–311++G(d,p) basis set with the help of Gaussian09 package program [64]. The molecular structure of B-DNA dodecamer (PDB Code: 1BNA) [67] having 1.9 Angstrom resolution was prepared as a target receptor before molecular docking analysis was realized. All water molecules and ions in the receptor file were removed and the polar hydrogens were added to receptor molecule. After ligand and receptor were determined and prepared, all pdb files were converted to pdbqt file format by AutoDockTools1.5.6 program [68]. The grid box was adjusted to $x = 40$ Å, $y = 40$ Å and $z = 40$ Å with 0.375 nm grid spacing. After all the adjustments were made, the molecular docking study was carried out with the AutoDock Vina 1.1.2 program [69]. The most favorable binding affinities, the close interactions and root mean square deviation (RMSD) values for D3 molecule were obtained as a result of the docking study performed. All pictures (close interactions and h-bonding interactions) were obtained using PyMol 2.2.3 [70] and AutoDockTools1.5.6 programs. Pharmacokinetic and toxicity profiles (ADMET properties) of D3 were determined by *Molinspiration* [71], *Swissadme* [72] and *PreADMET* [73] online servers.

2.2.7. Cell cultures

HeLa (human epithelial cervical cancer) and MCF-7 (human breast cancer) cell lines were cultured in DMEM (Sigma), containing 10% fetal bovine serum (FBS, Gibco Lab) and penicillin (100 IU/mL, İ.E. Ulagay), streptomycin (100 µg/mL, I.E. Ulagay). MAT-Lylu (rat prostate cancer) cell line was maintained in RPMI-1640 medium (Gibco Lab.) containing%1 FBS (Gibco Lab), 2 mM L-glutamine (Gibco Lab.) and 250 nM dexamethasone (Sigma) without antibiotics. MCF-7, HeLa and Mat-Lylu cell lines were incubated at 37 °C in a humid environment containing 5% CO_2.

2.2.8. Cell cytotoxicity assay

HeLa and MCF-7 cell lines were seeded at a density of 1 × 10^4 and MAT-Lylu cell line was seeded at a density of 5 × 10^3 per well in a 96-well cell culture plate for the MTT assay. Cells were incubated overnight, and different D3 concentrations added to wells. At the end of incubation period, 40 µL of MTT (5 mg/ml) were added to each well. Cells reincubated for 4 h and 160 µL of DMSO was added to each well to dissolve formazan crystals. Absorbance was measured using Elisa Reader at 450–690 nm. Percentage of the cell viability was calculated using Eq (4).

$$\text{Viability}\,\% = [(\text{Absorbance of Experimental Group}) / (\text{Absorbance of Control Group})] \times 100 \quad (4)$$

2.2.9. Statistical analysis

One-way analysis of variance (ANOVA) in the IBM SPSS Statistics 22 package program was used for statistical analysis of Ames test and DPPH antioxidant activity results. In addition, the results are presented as the mean ± SD of the triple measurement. The significance level of the group averages was determined at the $p<0.05$ level with the Tukey test. For statistical analysis of the cytotoxicity experiments, differences between control and treatment groups were evaluated by One-way ANOVA and Dunnett's multiple comparison tests using GraphPad Prism Software with a significance level of $p< 0.05$. (Prism Version 7.0; GraphPad Software, Inc.).

3. Results and discussion

3.1. Synthesis of D3

In this study, 7-hydroxy-8-(((1-hydroxy-3-phenylpropan-2-yl)imino)methyl)-4-(trifluoromethyl)-2*H*-chromen-2-one (**D3**) was prepared by the condensation reaction of 8-formyl-7-hydroxy-4-(trifluoromethyl)coumarin (**2**) with 2-amino-3-phenyl-1-propanol (Fig. 1). The structure and purity of the compound was determined by its spectral data (IR, NMR, LC, QTOF, Figs. S1–S4) and it was concluded that they are in accordance with the structure.

3.2. DNA binding assay results

DNA targeting is an important strategy in the treatment of various diseases. As DNA is the primary pharmacological target of antitumor drugs, for the design of new anticancer drug, the determination of interactions between the small drug molecule with CT-DNA is the one of the crucial method [74]. UV–vis absorption spectroscopy is a useful method to investigate the interaction between

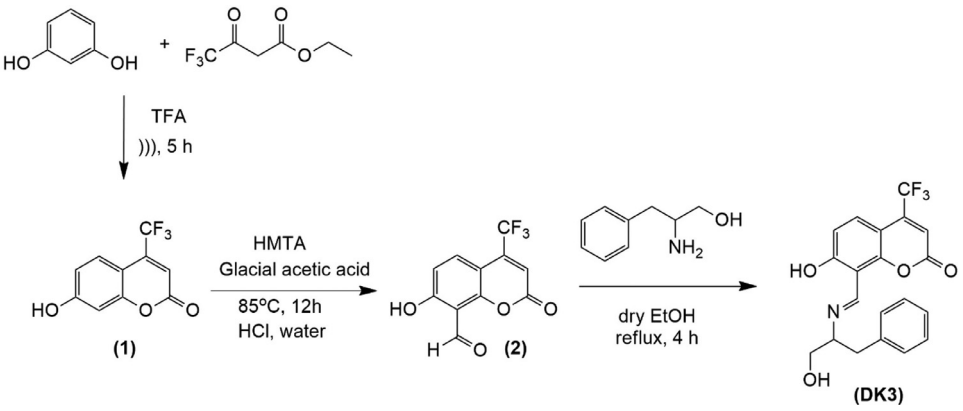

Fig. 1. Synthesis of D3.

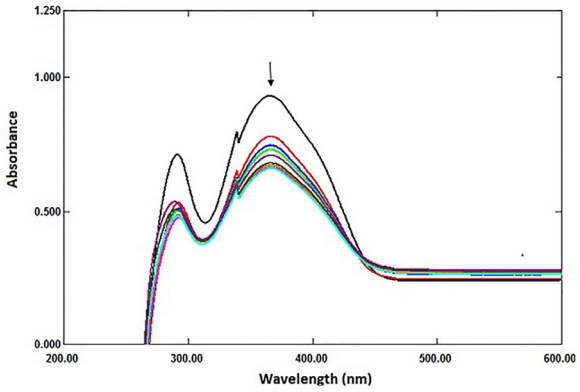

Fig. 2. The absorption spectra of D3 in the presence of increasing amounts of CT-DNA and in the absence of CT-DNA (black peak). Conditions: [DK3] = 30 μM, [DNA] = 0–270 μM. Arrow (↓) indicates absorbance changes upon increasing DNA concentration.

small drug molecules and CT-DNA, and it can be also obtained the information about interaction model [75–77]. The interaction is observed as a shift in absorbance (hypochromic, hyperchromic) or maximum wavelength (bathochromic, hypochromic) [78]. The absorption spectra of D3 in the presence and absence of CT-DNA were given in Fig. 2. It was seen from the figure, D3 exhibited a 29.1% hypochromic effect at 365 nm wavelength, and a 2 nm bathochromic (red) shift. Hypochromic effect and bathochromic shift indicate that D3 binds to DNA either via intercalation or groove binding [79–82].

Molecules, binds to the DNA by intercalation, are used in cancer treatment owing to inhibit DNA replication in fast-growing cancer cells [83,84]. Although these kinds of bound molecules do not have DNA sequence selectivity, studies have reported that they bind more to regions where guanine and cytosine are dense [85,86].. Molecules that bind to the groove, as well as molecules that bind to DNA by intercalation, have clinical importance as anticancer agents [87]. It was reported that molecules bind to the groove regions rich in adenine and thymine on the DNA [88]. It is desirable that molecules developed for cancer treatment are bound by intercalation or the groove. Our results showed D3 can exhibit both forms of binding.

The K_b value of D3 was found to be 4×10^5 M^{-1}. Although this value is lower than the classical intercalator (Ethidium bromide $K_b = 7 \times 10^7$ M^{-1}) [89], it coincides with the values in other studies that are stated to be linked to DNA by intercalation [75,76,89,90]. The Gibbs energy (ΔG) of D3 was determined using the Eq (5).

$$\Delta G = -RT \ln K \quad (5)$$

In the equation, "R" is the gas constant (8.314 J K^{-1} mol^{-1}) and T is the temperature (298 °K). As a result of the calculation, the Gibbs energy value was found to be −7.63 kcal / mol. The energy value calculated by the molecular docking study was found to be −7.9 kcal / mol. When the experimental and theoretical values were compared, the relative percentage error between the two values was determined as 3.4%. According to these results, it was determined that the interaction between D3 and DNA was spontaneous [58].

3.3. Mutagenity assay results

The crucial challenge of effective drugs developed for cancer treatment is their toxicity [91–93]. Today, the development of effective and safe drugs has been the primary goal of researchers. As the Ames test is one of the principal tools of toxicological genetics, it has become part of a series of pre-clinical tests to detect the mutagenic potential of new drugs [94]. The Ames/Salmonella test is the method used to identify chemicals that cause gene mutations. In this study, the D3 molecule, an imino coumarin derivative, was synthesized as an anticancer drug candidate, and for this purpose we evaluated to determine its safety. The mutagenicity of D3 was determined using *S. typhimurium* TA98 and TA100 strains. In this method, it is used that Salmonella strains that are unable to synthesize histidine due to mutations in the histidine operon and then cannot grow or form colonies in their absence. Chemicals / drug candidates with mutagenic potential can restore gene function. Thus, a positive result from the test indicates that chemical / drug candidate is mutagen [58]. In our study, four different concentrations of D3 (6.25, 12.5, 25 and 50 µg / Plate) were used. The results showed that the concentrations of D3 used were not mutagenic according to the method (Table 1, Figs. 3 and 4), and statistical analysis determined by Mortelman and Zeiger [95]. In addition, the results obtained coincide with the results of anti-cancer drug candidates in the literature [58,59,96,97].

3.4. Antioxidant activity results

Oxidative damage is being the main contributing factor to cancer formation and the development of cancer. Molecules with the ability to scavenge and reduce free radicals can exhibit chemo preventive activity [93,98,99]. Therefore, we evaluated the antioxidant activity of D3 in our study. The 2,2-diphenyl-1-picrylhydrazyl (DPPH) spectrophotometric method is one of the most widely applied method in order to assess the radical scavenging activity

Table 1
Mutagenity results of D3 ($n = 3$ for each set of conditions). Data are presented as mean ± standard deviation.

Treatment		Concentration (µg/Plate)	Number of revertant colony/Plate	
			TA98 Mean±SD	TA100 Mean±SD
D3		6.25	48.00 ± 7.00	156,00±3,60
		12.5	47.00±9.53	141,33±16,04
		25	57.66±1.52	141,00±3,60
		50	49.33±0.57	128,33±18,92
Positive	NPD	10	620.00±39.68*	
Control	SA	1		971,66±20.20*
Negative Control (DMSO)			49.00±3.00	138.33±27.00
Spontaneous Control			42.33±1.52	135.66±27.53

NPD: 4-Nitro-o-phenylenediamine.
SA: Sodium azide.
* The mean revertant colony number difference between negative control and application groups is significant at the level of $p < 0.05$ (Tukey test).

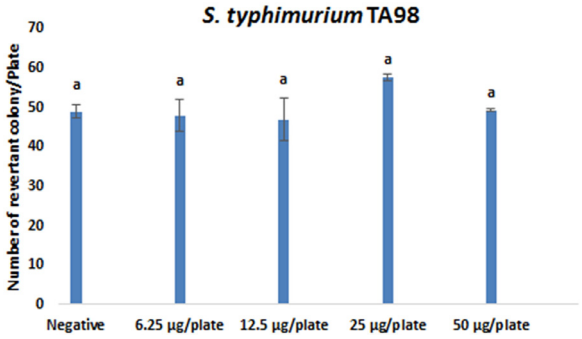

Fig. 3. Mutagenity results of D3 on S. typhimurium TA98. Data are presented as mean ± standard error ($p < 0.05$).

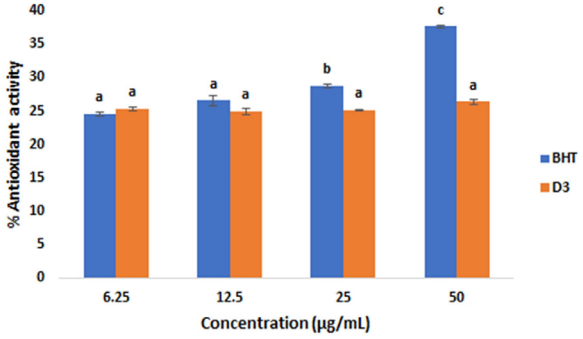

Fig. 5. Antioxidant activity of D3. Data are presented as mean ± standard error ($p < 0.05$).

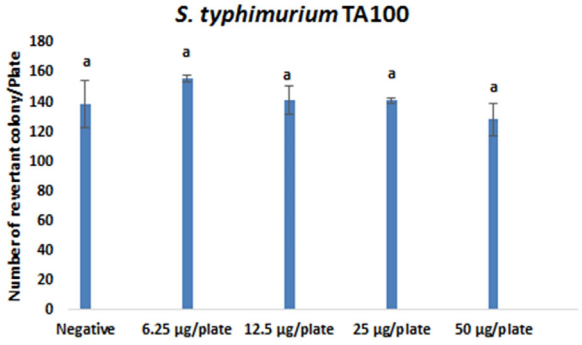

Fig. 4. Mutagenity results of D3 on S. typhimurium TA100. Data are presented as mean ± standard error ($p < 0.05$).

[100]. This method was used for assessment of the antioxidant activity of D3. According to this method, chemicals must have strong hydrogen donor groups to show good antioxidant properties [100].

The graphic of DPPH stable free radical scavenging activity of D3 is shown in Fig. 5. It was found that the antioxidant activity of D3 did not increase depending on the concentration, and the antioxidant activity of D3 was low compared to BHT. These results were also statistically supported ($P < 0.05$). As a result, it was found that all concentrations of D3 had antioxidant activity. It was thought that antioxidant activity may be due to the OH groups in the structure of D3 [100,101].

3.5. Frontier molecular orbitals analysis results

The Frontier Molecular Orbitals which enable identification of reactivity, optical and electronic properties of a molecule, are defined by HOMO / LUMO interactions. HOMO is the outermost molecule orbital occupied by electrons and acts as an electron donor, while LUMO is the first empty molecule orbital not occupied by electrons and has the characteristics of an electron acceptor. Besides, HOMO energy is related to the ionization potential, represents the ability to donate electrons, LUMO energy is related to electron affinity and characterizes the molecule's ability to receive electrons. The energy difference (ΔE) between HOMO and LUMO plays an important role in chemical reactions and expresses the chemical stability of the molecule. The closer the energy levels of the interacting molecular orbitals (from HOMO to LUMO), the smaller the ΔE energy difference; interaction and reaction occur more easily. The TDDFT/B3LYP 6-311++G(d, p) calculations were made to determine the difference (ΔE) between HOMO and LUMO energy values in two different environments (vacuum and water), depending on different ambient conditions. The frontier molecular orbitals and the energy gap (ΔE) of the compound obtained in two different environments (vacuum and water) was shown in Fig. 6. For vacuum, the HOMO orbitals were concentrated densely on the 2-amino-3-phenyl-1-propanol moiety, the OH group and the C–C bonds on the pyrone ring of the coumarin core LUMO orbitals have also been heavily located on coumarin ring. The calculated energy gap (ΔE) value was 3.91 eV. HOMO molecular orbitals are on all atoms except CF_3 group for water environment, while LUMO orbitals are located on only coumarin ring just like a vacuum environment. The calculated band gap (ΔE) for the water

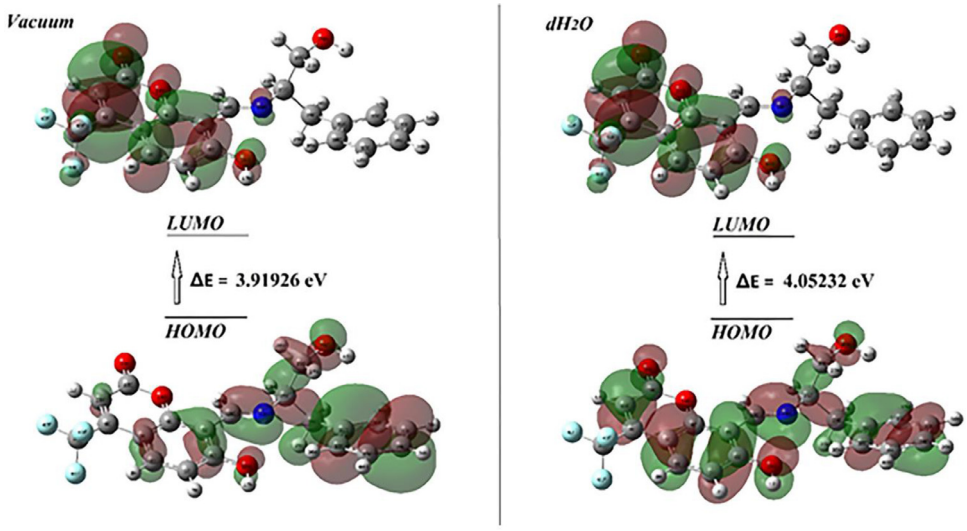

Fig. 6. The frontiers molecular orbitals and band gap energies for D3.

Table 2
Calculated molecular orbital energies (eV) and energy differences of D3.

TD-B3LYP/6-311++G(d,p)	E_{LUMO+1}	E_{LUMO}	E_{HOMO}	E_{HOMO-1}	$\Delta E_{HOMO-LUMO}$	$\Delta E_{(HOMO)-(LUMO+1)}$	$\Delta E_{(HOMO-1)-(LUMO)}$
Vacuum	−1.98181	−2.88631	−6.80557	−7.04177	3.91926	4.82376	4.15546
dH_2O	−1.80384	−2.70808	−6.76040	−6.90680	4.05232	4.95656	4.19872

Table 3
The calculated values of ionization potential, electron affinity, electronegativity, chemical hardness, chemical potential and ΔE (gap) for D3 in vacuum and dH2O.

Vacuum	TD-DFT/6311++G(d,p)	**Energy (a.u.)**	**Energy (eV)**
Homo Energy	E_{HOMO}	−0.25010	−6.80557
Lumo Energy	E_{LUMO}	−0.10607	−2.88631
Ionization potential	I= $-E_{HOMO}$	0.25010	6.80557
Electron affinity	A= - E_{LUMO}	0.10607	2.88631
Electronegativity	$\chi = (I + A)/2$	0.178085	4.84594
Chemical potential	$\mu = -(I + A)/2$	−0.178085	−4.84594
Chemical hardness	$\eta = (I-A)/2$	0.072015	1.95963
ΔE (gap)	E_{LUMO-} E_{HOMO}	0.14403	3.91926
dH_2O	**TD-DFT/6311++G(d,p)**	**Energy (a.u.)**	**Energy (eV)**
Homo Energy	E_{HOMO}	−0.24844	−6.76040
Lumo Energy	E_{LUMO}	−0.09952	−2.70808
Ionization potential	I= $-E_{HOMO}$	0.24844	6.76040
Electron affinity	A= - E_{LUMO}	0.09952	2.70808
Elektronegativity	$\chi = (I + A)/2$	0.17398	4.73424
Chemical potential	$\mu = -(I + A)/2$	−0.17398	−4.73424
Chemical hardness	$\eta = (I-A)/2$	0.07446	2.02616
ΔE (gap)	E_{LUMO-} E_{HOMO}	0.14892	4.05232

environment was 4.05 eV. Electron transitions in the D3 molecule for the vacuum environment were from the 2-amino-3-phenyl-1-propanol, OH group and the C–C bonds on the pyrone ring of coumarin core to the coumarin ring. For the D3 molecule in the water environment, electron transfer within the molecule is towards coumarin ring from all molecules except the CF_3 group. The calculated molecular orbital energies (eV) and energy differences of D3 were tabulated in Table 2.

The ionization potential (I=- E_{HOMO}) = 6.80 eV, 6.76 eV, electron affinity (A=- E_{LUMO}) = 2.88 eV, 2.70 eV, the electronegativity ($\chi = (I + A)/2$) = 4.84 eV, 4.73 eV, chemical potential ($\mu = -(I + A)/2$) = *−4.84 eV, −4.73 eV* and chemical hardness ($\eta = (I - A)/2$) = 1.95 eV, 2.02 eV values were performed for D3 in vacuum and dH_2O environment, respectively, and tabulated in Table 3. As can be seen from Table 3, the chemical hardness degree of the D3 molecule in the polar water environment increased compared to the vacuum environment, and therefore, the chemical stability also increased with the HOMO LUMO band gap. The calculated UV–vis absorption wavelengths λ (nm), excitation energies E (eV) and oscillator strengths (*f*) of **D3** in vacuum and dH_2O were depicted in Fig. S5 and tabulated in Table 4. The greatest contributions for UV–vis transitions come from HOMO-LUMO with 89% and 76% major contributions for vacuum and water environment with excitation energy of 3.53 eV and 3.63 eV and excitation wavenumber of 350.5 nm and 340.6 nm, respectively.

3.6. Molecular docking and ADMET results

In order to reveal the interaction of the D3 molecule with DNA, 9 different conformation of the D3 molecule bound to the B-DNA dodecamer structure were identified and the most stable binding pose and energy among them were determined by molecular docking analysis. The best binding pose which corresponds to the best binding affinity value (−7.9 kcal / mol) and other poses of the D3 molecule and RMSD values of these were given in Table 5. The hydrogen bonding and close interactions between D3 and B-DNA were also tabulated in Table 6a and b.

By looking at the close interactions, it was observed that the adenines and guanines belonging to DNA and the D3 molecule interact. DG10, DG16 (deoxyguanosines), DA17, DA18 (deoxyadenosine), which have close interactions with D3, have been seen to be capable of hydrogen bonding with D3 (cf. Figs. 7 and 8). It was seen that the D3 molecule interacts with DNA, as seen in Fig. 8.

A closer look at the hydrogen bonds reveals that the O1 atom of D3 and the hydrogen atom bound to the nitrogen of D3 come to the fore. Hydrogen bonds are of great importance in receptor ligand interactions as they provide high stability and strong binding. In this study, it was seen that the O1 atom of D3 molecule made hydrogen bond with H3 (2.4 Å) and H22 (2.3 Å) of DG10 and H21 (3.1 Å) and H22 (2.1 Å) of DG16. Additionally, it was seen that hydrogen atom bound to the nitrogen (HN1) of D3 molecule made hydrogen bond with O3' (2.6 Å) and O4' (3.2 Å) of DA17. The

Table 4
Calculated absorption wavelengths λ (nm), excitation energies E (eV) and oscillator strengths (f) of D3 along with transition levels and assignments in vacuum and dH2O.

TD-B3LYP/6-311++G(d,p)	E (eV)	λ (nm)	*f*	major contribs.		symmetry
dH$_2$O	3.6393	340.68	0.0741	H-3→L	(13%)	Singlet-A
				H→L	(76%)	
	3.8009	326.2	0.3104	H-3→L	(16%)	Singlet-A
				H-1→L	(62%)	
				H→L	(15%)	
	3.8636	320.9	0.0002	H-4→L	(51%)	Singlet-A
				H-2→L	(36%)	
Vacuum	3.5374	350.5	0.0079	H→L	(89%)	Singlet-A
	3.6907	335.94	0.0002	H-3→L	(48%)	Singlet-A
				H-2→L	(15%)	Singlet-A
				H-1→L	(23%)	Singlet-A
	3.8089	325.51	0.0199	H-4→L	(48%)	Singlet-A
				H-1→L	(31%)	Singlet-A

Table 5
The affinity energies and RMSD values of D3 bounded by B-DNA dodecamer.

Mode	Affinity kcal/mol	Dist from rmsd l.b.	Best mode rmsd l.b.
1	−7.9	0.000	0.000
2	−7.8	1.125	3.131
3	−7.6	3.983	8.364
4	−7.6	3.941	8.060
5	−7.5	4.057	8.170
6	−7.5	1.249	1.883
7	−7.5	4.074	8.081
8	−7.4	4.078	8.534
9	−7.4	4.008	8.479

Table 6
(a). The close interactions, binding affinity and hydrogen bonding between D3 and B-DNA (b). The hydrogen bonding interactions of D3 bounded by B-DNA dodecamer.

Table 6a

Affinity (kcal/mol)	**Close interactions**	**Hydrogen bonding (Å)**
−7.9	DG10, DG16, DA17, DA18	DG10, DG16, DA17, DA18

Table 6b

DNA Chain	Residues of DNA	Atom Number of Residues of DNA	Atom Number of D3	Interaction (Å)
A	DG10	H3	O1	2.4
A	DG10	H22	O1	2.3
B	DG16	H21	O1	3.1
B	DG16	H22	O1	2.1
B	DG16	H22	O2	3.4
B	DA17	O3‘	HN1	2.6
B	DA17	O4‘	HN1	3.2
B	DA18	OP1	H2	3.4

best docked pose of D3 with the B-DNA and preferable hydrogen bonding interactions were shown in Figs. 7 and 8, respectively. Determining ADME features, which is an important step in drug development studies, gives information about the pharmacokinetics of drug candidate molecules. The ADME profile of the drug provides vital information about the easy absorbability of the drug when taken by mouth, its transport to the target area in the body and its removal. Determination of many features such as molecular weight, brain / blood partition coefficient, skin permeability helps to develop effective drugs. Lipinski's 5 rules also provide information on the appropriateness of oral administration of drug candidate molecules. Four simple physicochemical parameters were determined by Lipinski according to the active drugs that passed to the phase II clinical stage [102,103]. PSA (Polar Surface Area) is an important parameter that characterizes the transport of drug molecules. The PSA value to be used as a substitute for BBB penetration is expected to be less than 90 Å^2 [104–106]. According to the results in the Table S1, two online server systems (*Molinspiration* and *Swissadme*) set PSA value as 83.03 Å^2 for D3. Also, according to the *Swissadme* and *PreADMET* (in Table S2) online servers, the synthesized D3 molecule is a molecule with high compliance with Lipinski rules. Additionally, gastrointestinal (GI) absorption of D3 is high. In the literature, the range of Caco-2 permeability is given as $<1 \times 10^{-6}$ cm/sec (0–20% poor), $1–10 \times 10^{-6}$ cm/sec (20–70% moderate), $>10 \times 10^{-6}$ cm/sec (70–100% good), respectively [107,108]. Using the *PreADMET* online server, the Caco-2 permeability of D3 was determined as 20.7612 nm/sec with moderate value. The calculated human intestinal absorption (HIA) value was 94,058,651%. The percentage of plasma protein binding, which is important in the transport of drugs, is 87,813,153. According to WDI (World Drug Index) measurement [109], D3 molecule is in 90% cutoff. CMC like rule [110], which is similar to the rule of 5, is qualified for D3 molecule. The calculated drug-likeliness and ADMET features of D3 molecule were given in Tables S1 and S2. According to all the interpreted results, the D3 molecule was seen as an important drug candidate

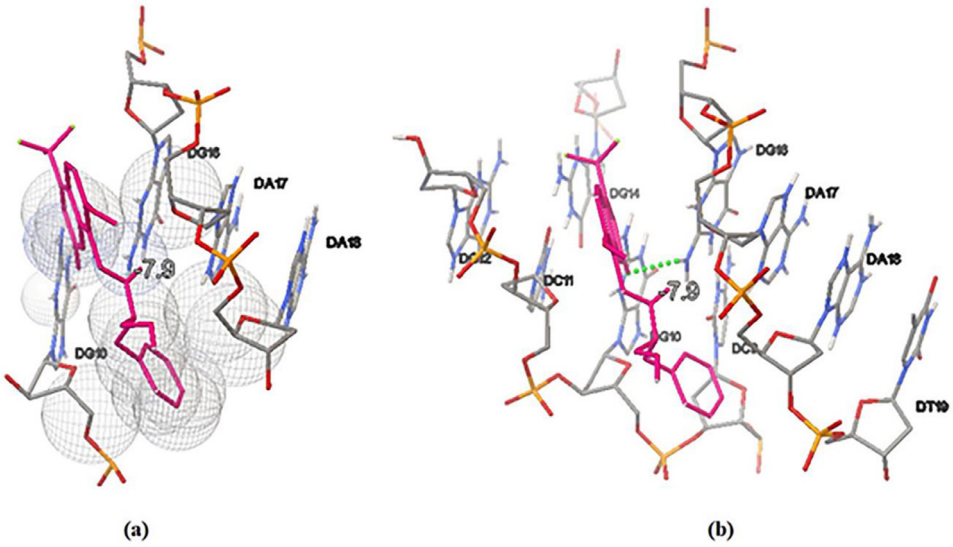

Fig. 7. The best docked pose and close interaction between D3 and the B-DNA.

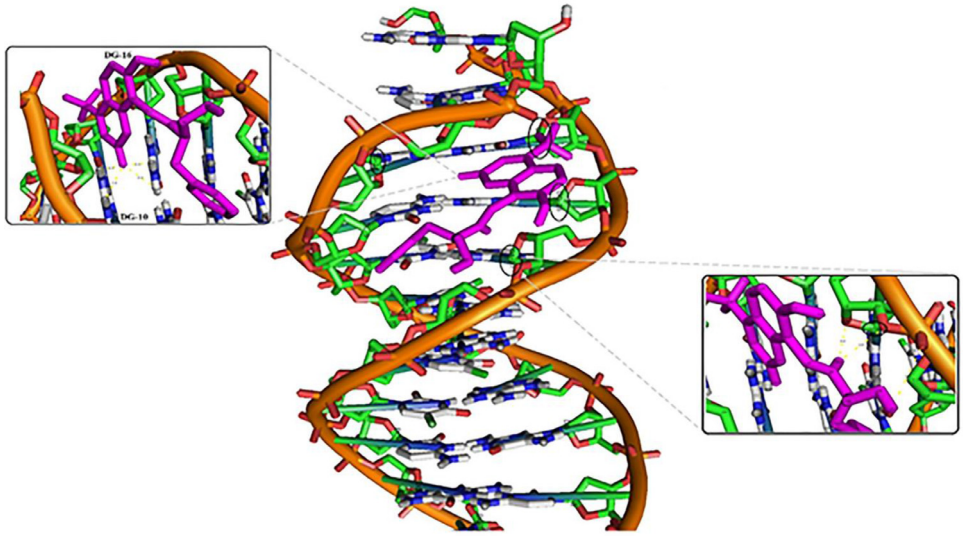

Fig. 8. The preferable hydrogen bonding interactions between D3 and the B-DNA.

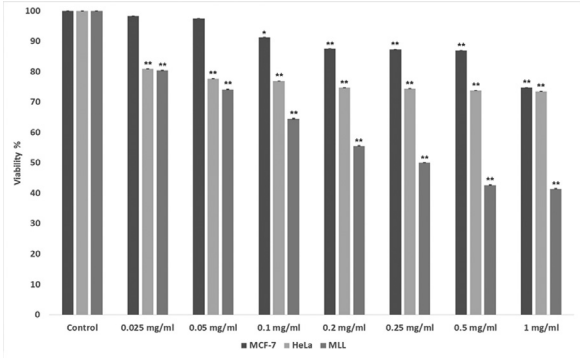

Fig. 9. Effect of different D3 concentrations on the viability of MCF-7, HeLa and MAT-Lylu cell lines after 24 h treatment (* $p<0.05$ vs control, ** $p<0.01$ vs control).

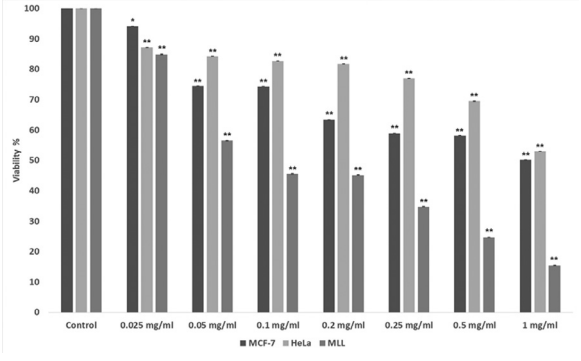

Fig. 10. Effect of different D3 concentrations on the viability of MCF-7, HeLa and MAT-Lylu cell lines after 48 h treatment (* $p<0.05$ vs control, ** $p<0.01$ vs control).

3.7. Cell cytotoxicity assay

HeLa, MCF-7 and MAT-Lylu cell lines were treated with different concentrations of D3 (0.025, 0.05, 0.1, 0.2, 0.25, 0.5 and 1 mg/ml) and cytotoxicity was measured via MTT assay after 24 and 48 h of incubation. As shown in Fig. 9 for 24 h and Fig. 10 for 48 h D3 has a cytotoxic effect on all cell lines. IC_{50} values for D3 in MAT-Lylu cell line was 0.25 mg/ml in the 24 h experimental group. IC_{50} val-

ues of HeLa and MCF-7 cells were determined as 1 mg/ml for both cell lines in the 48 h experimental group. Comparison of cytotoxicity between cancer cells, it was determined that D3 showed the highest cytotoxic activity in MAT-Lylu cell lines. According to the results 0.025 and 0.05 concentrations did not show any cytotoxic activity in MCF-7 cells in the 24 h experimental group ($p>0.05$) (Fig. 9) and for 48 h, all concentrations have a toxic effect on both cell lines as compared with the control group (Fig. 10). In addition, it was found that MCF-7 and MAT-Lylu cell lines showed a concentration-dependent decrease in cell viability.

4. Conclusion

Nowadays, it is known that the length and high costs of new drug development processes are among the biggest problems of the pharmaceutical industry. Computer-aided drug design has emerged as a promising new science in this sense. In this study, a new iminocoumarin derivative (D3) was designed and synthesized as a new anti-cancer drug molecule. DNA binding activity of D3 molecule was evaluated experimentally and theoretically by DNA binding assays and molecular docking analysis method. Adenine and guanine bases of DNA more interact with the D3 molecule and this interaction was achieved through the hydrogen bonds that provide high stability and strong binding (−7.9 kcal/mol) energy. The experimental Gibbs free energy value was observed as −7.63 kcal / mol. The results of binding assay and in silico studies revealed that two values were very close to each other and thus the interaction between D3 and DNA was spontaneous. The synthesized D3 molecule, with its calculated high gastrointestinal (GI) absorption value, appropriate PSA value, high absorption human intestine (HIA) value, and the high percentage of binding to plasma protein value, showed high compliance with Lipinski rules and has the potential to be a drug due to its promising pharmacokinetic and ADME properties. Anticancer activity of D3 was examined on three cancer cell lines, including MCF-7, HeLa and MAT-Lylu. It was found that D3 decreased cell viability, depending on concentration and time. Moreover, it was determined that D3 showed higher cytotoxicity on the MAT-Lylu cell lines compared to MCF-7 and HeLa cell lines. All these results suggest that D3 may be used as an anticancer drug in the future.

Declaration of Competing Interest

The authors declare that they have no known competing financial interests or personal relationships that could have appeared to influence the work reported in this paper.

CRediT authorship contribution statement

Serda Kecel-Gunduz: Data curtion, Supervision, Writing – review & editing. **Yasemin Budama-Kilinc:** Supervision, Writing – review & editing. **Bahar Gok:** Data curtion, Writing – review & editing. **Bilge Bicak:** Data curtion, Methodology, Writing – review & editing. **Gizem Akman:** Data curtion, Writing – review & editing. **Busra Arvas:** Data curtion, Writing – review & editing. **Feray Aydogan:** Data curtion, Supervision, Writing – review & editing. **Cigdem Yolacan:** Data curtion, Supervision, Writing – review & editing.

Acknowledgement

This work was supported by Yildiz Technical University Scientific Research Foundation (project number FBA-2017-3168). In this study, the infrastructure of Applied Nanotechnology and Antibody Production Laboratory established with TUBITAK support (project numbers: 115S132 and 117S097) was used. Authors would thank to TUBITAK for their support.

Supplementary materials

Supplementary material associated with this article can be found, in the online version, at doi:10.1016/j.molstruc.2021.130539.

References

[1] Y.K. Al-Majedy, A.A.H. Kadhum, A.A. Al-Amiery, A.B. Mohamad, Coumarins: the antimicrobial agents, System. Rev. Pharm. 8 (1) (2017) 62.
[2] K.M. Amin, S.M. Abou-Seri, R.M. Abdelnaby, H.S. Rateb, M.A. Khalil, M.M. Hussein, Synthesis and biological evaluation of novel coumarin derivatives as potential antimicrobials agents, (2016).
[3] P. Jain, H. Joshi, Coumarin: chemical and pharmacological profile, J. Appl. Pharm. Sci. 2 (6) (2012) 236–240.
[4] K. Kasperkiewicz, M.B. Ponczek, J. Owczarek, P. Guga, E. Budzisz, Antagonists of vitamin K—popular coumarin drugs and new synthetic and natural coumarin derivatives, Molecules 25 (6) (2020) 1465.
[5] O. Kayser, H. Kolodziej, Antibacterial activity of simple coumarins: structural requirements for biological activity, Z. Naturforsch. 54c (3–4) (1999) 169–174.
[6] K.M. Khan, Z.S. Saify, M.Z. Khan, Zia-Ullah, M.I. Choudhary, Atta-ur-Rahman, S. Perveen, Z.H. Chohan, C.T. Supuran, Synthesis of coumarin derivatives with cytotoxic, antibacterial and antifungal activity, J. Enzyme Inhib. Med. Chem. 19 (4) (2004) 373–379.
[7] J.T. Konc, E. Hejchman, H. Kruszewska, I. Wolska, D. Maciejewska, Synthesis and pharmacological activity of O-aminoalkyl derivatives of 7-hydroxycoumarin, Eur. J. Med. Chem. 46 (6) (2011) 2252–2263.
[8] I. Kostova, Synthetic and natural coumarins as cytotoxic agents, Curr. Med. Chem.-Anti-Cancer Agents 5 (1) (2005) 29–46.
[9] S. Mishra, A. Pandey, S. Manvati, Coumarin: an emerging antiviral agent, Heliyon 6 (1) (2020) e03217.
[10] C. Montagner, S.M. de Souza, C. Groposo, F. Delle Monache, E.F. Smânia, A. Smânia Jr., Antifungal activity of coumarins, Z. Naturforsch. 63c (1–2) (2008) 21–28.
[11] L. Wu, X. Wang, W. Xu, F. Farzaneh, R. Xu, The structure and pharmacological functions of coumarins and their derivatives, Curr. Med. Chem. 16 (32) (2009) 4236–4260.
[12] A. Sabt, O.M. Abdelhafez, R.S. El-Haggar, H.M. Madkour, W.M. Eldehna, E.E.-D.A. El-Khrisy, M.A. Abdel-Rahman, L.A. Rashed, Novel coumarin-6-sulfonamides as apoptotic anti-proliferative agents: synthesis, in vitro biological evaluation, and QSAR studies, J. Enzyme Inhib. Med. Chem. 33 (1) (2018) 1095–1107.
[13] J. Dandriyal, R. Singla, M. Kumar, V. Jaitak, Recent developments of C-4 substituted coumarin derivatives as anticancer agents, Eur. J. Med. Chem. 119 (2016) 141–168.
[14] K.M. Amin, A.M. Taha, R.F. George, N.M. Mohamed, F.F. Elsenduny, Synthesis, antitumor activity evaluation, and DNA-binding study of coumarin-based agents, Arch. Pharm. 351 (1) (2018) 1700199.
[15] J. Klenkar, M. Molnar, Natural and synthetic coumarins as potential anticancer agents, J. Chem. Pharm. Res. 7 (7) (2015) 1223–1238.
[16] X.F. Song, J. Fan, L. Liu, X.F. Liu, F. Gao, Coumarin derivatives with anticancer activities: an update, Arch. Pharm. 353 (8) (2020) e2000025.
[17] D. Cao, Y. Liu, W. Yan, C. Wang, P. Bai, T. Wang, M. Tang, X. Wang, Z. Yang, B. Ma, Design, synthesis, and evaluation of in vitro and in vivo anticancer activity of 4-substituted coumarins: a novel class of potent tubulin polymerization inhibitors, J. Med. Chem. 59 (12) (2016) 5721–5739.
[18] G. Luo, M. Muyaba, W. Lyu, Z. Tang, R. Zhao, Q. Xu, Q. You, H. Xiang, Design, synthesis and biological evaluation of novel 3-substituted 4-anilino–coumarin derivatives as antitumor agents, Bioorg. Med. Chem. Lett. 27 (4) (2017) 867–874.
[19] R. Miri, M. Nejati, L. Saso, F. Khakdan, B. Parshad, D. Mathur, V.S. Parmar, M.E. Bracke, A.K. Prasad, S.K. Sharma, Structure–activity relationship studies of 4-methylcoumarin derivatives as anticancer agents, Pharm. Biol. 54 (1) (2016) 105–110.
[20] S.A. Morsy, A.A. Farahat, M.N. Nasr, A.S. Tantawy, Synthesis, molecular modeling and anticancer activity of new coumarin containing compounds, Saudi Pharm. J. 25 (6) (2017) 873–883.
[21] M.A. Musa, V.L. Badisa, L.M. Latinwo, J. Cooperwood, A. Sinclair, A. Abdullah, Cytotoxic activity of new acetoxycoumarin derivatives in cancer cell lines, Anticancer Res. 31 (6) (2011) 2017–2022.
[22] A. Pangal, J. Shaikh, E. Khan, Current developments of C3-substituted coumarin hybrids as anti-cancer agents, Int. J. Pharm. Sci. Rev. Res. 42 (2017) 161–168.
[23] K.-G. Weng, Y.-L. Yuan, Synthesis and evaluation of coumarin derivatives against human lung cancer cell lines, Braz. J. Med. Biol. Res. 50 (11) (2017).
[24] A.A.H. Kadhum, A.A. Al-Amiery, A.Y. Musa, A.B. Mohamad, The antioxidant activity of new coumarin derivatives, Int. J. Mol. Sci. 12 (9) (2011) 5747–5761.
[25] Y.K. Al-Majedy, D.L. Al-Duhaidahawi, K.F. Al-Azawi, A.A. Al-Amiery, A.A.H. Kadhum, A.B. Mohamad, Coumarins as potential antioxidant agents complemented with suggested mechanisms and approved by molecular modeling studies, Molecules 21 (2) (2016) 135.
[26] M. Molnar, B. Šarkanj, M. Čačić, L. Gille, I. Strelec, Antioxidant properties and growth-inhibitory activity of coumarin Schiff bases against common foodborne fungi, Der Pharma Chem. 6 (6) (2014) 313–320.

[27] B. Parshad, A. Duraisamy, S. Saini, P. Yadav, P. Vats, K. Sunil, Synthesis and SAR study of antioxidant potential of polyhydroxy coumarin derivatives, Med. Chem. 6 (2016) 506–514.
[28] S. Rouaiguia-Bouakkaz, A. Benayahoum, The antioxidant activity of 4-hydroxycoumarin derivatives and some sulfured analogs, J. Phys. Org. Chem. 28 (12) (2015) 714–722.
[29] G. Tataringa, C. Stan, C. Mircea, A. Jitareanu, A.-M. Zbancioc, Antioxidant evaluation of some coumarin derivatives, Farmacia 64 (4) (2016) 533–538.
[30] Y. Al-Majedy, A. Al-Amiery, A.A. Kadhum, A. BakarMohamad, Antioxidant activity of coumarins, Syst. Rev. Pharm. 8 (1) (2017) 24.
[31] R.K. Arora, N. Kaur, Y. Bansal, G. Bansal, Novel coumarin–benzimidazole derivatives as antioxidants and safer anti-inflammatory agents, Acta Pharm. Sin. B 4 (5) (2014) 368–375.
[32] L. Han, B. Huang, Z. Xiong, C. Yan, One-pot synthesis of potential antioxidant agents, 3-carboxylate coumarin derivatives, J. Med. Plants Res. 9 (13) (2015) 435–444.
[33] R.G. Shinde, A.A. Khan, A. Barik, Coumarin derivatives with antioxidant and anticancer potential: a review, Int. J. Med. Appl. Sci. 3 (2014) 165–184.
[34] A. Makowska, L. Wolff, F. Sączewski, P. Bednarski, A. Kornicka, Synthesis and cytotoxic evaluation of benzoxazole/benzothiazole-2-imino-coumarin hybrids and their coumarin analogues as potential anticancer agents, Pharmazie. 74 (11) (2019) 648–657.
[35] R. Mladenova, M. Ignatova, N. Manolova, T. Petrova, I. Rashkov, Preparation, characterization and biological activity of Schiff base compounds derived from 8-hydroxyquinoline-2-carboxaldehyde and Jeffamines ED®, Eur. Polym. J. 38 (5) (2002) 989–999.
[36] G. Murugavel, T. Punniyamurthy, Novel copper-catalyzed multicomponent cascade synthesis of iminocoumarin aryl methyl ethers, Org. Lett. 15 (15) (2013) 3828–3831.
[37] S. Pandeya, D. Sriram, G. Nath, E. DeClercq, Synthesis, antibacterial, antifungal and anti-HIV activities of Schiff and Mannich bases derived from isatin derivatives and N-[4-(4′-chlorophenyl) thiazol-2-yl] thiosemicarbazide, Eur. J. Pharm. Sci. 9 (1) (1999) 25–31.
[38] P. Panneerselvam, R.R. Nair, G. Vijayalakshmi, E.H. Subramanian, S.K. Sridhar, Synthesis of Schiff bases of 4-(4-aminophenyl)-morpholine as potential antimicrobial agents, Eur. J. Med. Chem. 40 (2) (2005) 225–229.
[39] N. Vukovic, S. Sukdolak, S. Solujic, N. Niciforovic, Substituted imino and amino derivatives of 4-hydroxycoumarins as novel antioxidant, antibacterial and antifungal agents: synthesis and in vitro assessments, Food. Chem. 120 (4) (2010) 1011–1018.
[40] M.S. Al-Said, M.G. El-Gazzar, M.M. Ghorab, In-vitro cytotoxic and radiosensitizing evaluation of novel 2-pyridone, isoquinoline, chromene and chromenopyridone derivatives, Eur. J. Chem. 3 (2) (2012) 228–234.
[41] M. Costa, F. Areias, L. Abrunhosa, A. Venâncio, F. Proença, The condensation of salicylaldehydes and malononitrile revisited: synthesis of new dimeric chromene derivatives, J. Org. Chem. 73 (5) (2008) 1954–1962.
[42] K. Douadi, S. Chafaa, T. Douadi, M. Al-Noaimi, I. Kaabi, Azoimine quinoline derivatives: synthesis, classical and electrochemical evaluation of antioxidant, anti-inflammatory, antimicrobial activities and the DNA/BSA binding, J. Mol. Struct. 1217 (2020) 128305.
[43] C. Ozluer, H.E.S. Kara, In vitro DNA binding studies of anticancer drug idarubicin using spectroscopic techniques, J. Photochem. Photobiol. B 138 (2014) 36–42.
[44] S. Lee, K. Sivakumar, W.-S. Shin, F. Xie, Q. Wang, Synthesis and anti-angiogenesis activity of coumarin derivatives, Bioorg. Med. Chem. Lett. 16 (17) (2006) 4596–4599.
[45] H. Perumalsamy, K. Sankarapandian, K. Veerappan, S. Natarajan, N. Kandaswamy, L. Thangavelu, S.R. Balusamy, In silico and in vitro analysis of coumarin derivative induced anticancer effects by undergoing intrinsic pathway mediated apoptosis in human stomach cancer, Phytomedicine 46 (2018) 119–130.
[46] R.K. Singh, T.S. Lange, K.K. Kim, L. Brard, A coumarin derivative (RKS262) inhibits cell-cycle progression, causes pro-apoptotic signaling and cytotoxicity in ovarian cancer cells, Invest. New Drugs 29 (1) (2011) 63–72.
[47] B. Omarbasha, W. Heston, R. Huryk, W. Fair, Treatment of metastatic prostate derived tumor with cimetidine and coumarin, J. Urol. 139 (1988) 176.
[48] B. Omarbasha, W. Heston, R. Huryk, W. Fair, Decrease prostatic size in response to coumarin treatment, in: Proceedings Of The American Association For Cancer Research, 1988, p. 372. Amer Assoc Cancer Research 615 Chestnut St, 17th Floor, Philadelphia, Pa.
[49] Y. Eker, E. Şenkuytu, Z. Ölçer, T. Yıldırım, G.Y. Çiftçi, Novel coumarin cyclotriphosphazene derivatives: synthesis, characterization, DNA binding analysis with automated biosensor and cytotoxicity, J. Mol. Struct. 1209 (2020) 127971.
[50] E.H. Maleki, A.R. Bahrami, H. Sadeghian, M.M. Matin, Discovering the structure–activity relationships of different O-prenylated coumarin derivatives as effective anticancer agents in human cervical cancer cells, Toxicol. In Vitro. 63 (2020) 104745.
[51] R. Corvi, F. Madia, In vitro genotoxicity testing–can the performance be enhanced? Food Chem. Toxicol. 106 (2017) 600–608.
[52] Food and Drug Administration, HHS., in: International Conference on Harmonisation; Guidance on S2 (R1) Genotoxicity Testing and Data Interpretation for Pharmaceuticals Intended for Human Use; Availability. Notice, 77, Federal register, 2012, pp. 33748–33749. Notice, Federal register.
[53] Guideline I.H.T., Guidance on genotoxicity testing and data interpretation for pharmaceuticals intended for human use S2 (R1), in: International Conference on Harmonization of Technical Requirements for Registration of Pharmaceuticals for Human Use, ICH Expert Working Group, 2011, pp. 1–25.
[54] Z. Hajisharifi, M. Piryaiee, M. Mohammad Beigi, M. Behbahani, H. Mohabatkar, Predicting anticancer peptides with Chou's pseudo amino acid composition and investigating their mutagenicity via Ames test, J. Theor. Biol. 341 (2014) 34–40.
[55] A. Kulkarni, S.A. Patil, P.S. Badami, Synthesis, characterization, DNA cleavage and in vitro antimicrobial studies of La (III), Th (IV) and VO (IV) complexes with Schiff bases of coumarin derivatives, Eur. J. Med. Chem. 44 (7) (2009) 2904–2912.
[56] J.M. Timonen, R.M. Nieminen, O. Sareila, A. Goulas, L.J. Moilanen, M. Haukka, P. Vainiotalo, E. Moilanen, P.H. Aulaskari, Synthesis and anti-inflammatory effects of a series of novel 7-hydroxycoumarin derivatives, Eur. J. Med. Chem. 46 (9) (2011) 3845–3850.
[57] Y.-J. Liu, Z.-H. Liang, Z.-Z. Li, J.-H. Yao, H.-L. Huang, Cellular uptake, cytotoxicity, apoptosis, antioxidant activity and DNA binding of polypyridyl ruthenium (II) complexes, J. Organomet. Chem. 696 (14) (2011) 2728–2735.
[58] M. Tariq, N. Muhammad, S. Ali, J.H. Shirazi, M.N. Tahir, N. Khalid, Synthesis, spectroscopic, X-ray crystal structure, biological and DNA interaction studies of organotin (IV) complexes of 2-(4-ethoxybenzylidene) butanoic acid, Spectrochim. Acta Part A 122 (2014) 356–364.
[59] W.-C. Tsai, H.-C. Chang, Y.-H. Tseng, H.-Y. Yin, J.-W. Liao, D.C. Agrawal, H.-W. Wen, Toxicity evaluation of water extract of tissue-cultured Taraxacum formosanum by acute, subacute administration, and Ames test, Electron. J. Biotechnol. 45 (2020) 38–45.
[60] D. Gatehouse, P. Wilcox, R. Forster, I. Rowland, R. Callander, Bacterial mutation assays, in: Basic Mutagenicity Tests: UKEMS Part 1, 1990, pp. 13–61.
[61] D. Akin, Y. Durak, A. Uysal, E. Gunes, M.O. Aladag, Assessment of antimutagenic action of Celtis glabrata Steven ex Planch.(Cannabaceae) extracts against base pair exchange and frame shift mutations on Salmonella typhimurium TA98 and TA100 strains by Ames test, Drug Chem. Toxicol. 39 (3) (2016) 312–321.
[62] A.A. Shanty, J.E. Philip, E.J. Sneha, M.R.P. Kurup, S. Balachandran, P.V. Mohanan, Synthesis, characterization and biological studies of Schiff bases derived from heterocyclic moiety, Bioorg. Chem. 70 (2017) 67–73.
[63] W. Brand-Williams, M.-E. Cuvelier, C. Berset, Use of a free radical method to evaluate antioxidant activity, LWT-Food Sci. Technol. 28 (1) (1995) 25–30.
[64] M. Frisch, G. Trucks, H. Schlegel, G. Scuseria, M. Robb, J. Cheeseman, G. Scalmani, V. Barone, B. Mennucci, G. Petersson, in: Gaussian 09, 32, Gaussian, Inc, Wallingford, CT, 2009, pp. 5648–5652.
[65] E. Runge, E. Gross, Density-functional theory for time-dependent systems, Phys. Rev. Lett. 52 (1984) 997.
[66] S. Lehtola, Automatic algorithms for completeness-optimization of Gaussian basis sets, J Comput Chem 36 (5) (2015) 335–347.
[67] H.R. Drew, R.M. Wing, T. Takano, C. Broka, S. Tanaka, K. Itakura, R.E. Dickerson, Structure of a B-DNA dodecamer: conformation and dynamics, Proc. Natl. Acad. Sci. 78 (4) (1981) 2179–2183.
[68] G.M. Morris, R. Huey, W. Lindstrom, M.F. Sanner, R.K. Belew, D.S. Goodsell, A.J. Olson, AutoDock4 and AutoDockTools4: automated docking with selective receptor flexibility, J. Comput. Chem. 30 (16) (2009) 2785–2791.
[69] O. Trott, A.J. Olson, AutoDock Vina: improving the speed and accuracy of docking with a new scoring function, efficient optimization, and multithreading, J. Comput. Chem. 31 (2) (2010) 455–461.
[70] W.L. DeLano, Pymol: an open-source molecular graphics tool, CCP4 Newslett. Protein Crystallogr. 40 (1) (2002) 82–92.
[71] Molinspiration cheminformatics free web services, 2020, https://www.molinspiration.com.
[72] A. Daina, O. Michielin, V. Zoete, SwissADME: a free web tool to evaluate pharmacokinetics, drug-likeness and medicinal chemistry friendliness of small molecules, Sci. Rep. 7 (2017) 42717.
[73] S.K. Lee, G.S. Chang, I.H. Lee, J.E. Chung, K.Y. Sung, K.T. No, The PreADME: pc-based program for batch prediction of adme properties, EuroQSAR 9 (2004) 5–10.
[74] S. Tabassum, A. Asim, F. Arjmand, M. Afzal, V. Bagchi, Synthesis and characterization of copper (II) and zinc (II)-based potential chemotherapeutic compounds: their biological evaluation viz. DNA binding profile, cleavage and antimicrobial activity, Eur. J. Med. Chem. 58 (2012) 308–316.
[75] B. Coban, U. Yildiz, A. Sengul, Synthesis, characterization, and DNA binding of complexes [Pt (bpy)(pip)] 2+ and [Pt (bpy)(hpip)] 2+, JBIC J. Biol. Inorg. Chem. 18 (4) (2013) 461–471.
[76] K. Mahmood, W. Hashmi, H. Ismail, B. Mirza, B. Twamley, Z. Akhter, I. Rozas, R.J. Baker, Synthesis, DNA binding and antibacterial activity of metal (II) complexes of a benzimidazole Schiff base, Polyhedron 157 (2019) 326–334.
[77] C.-Y. Zhou, J. Zhao, Y.-B. Wu, C.-X. Yin, Y. Pin, Synthesis, characterization and studies on DNA-binding of a new Cu (II) complex with N1, N8-bis (l-methyl-4-nitropyrrole-2-carbonyl) triethylenetetramine, J. Inorg. Biochem. 101 (1) (2007) 10–18.
[78] M. Bhowon, S.B. Moosun, S. Jhaumeer-Laulloo, E.C. Hosten, T.I.A. Gerber, Transit. Met. Chem. 40 (2015) 445–458.
[79] Z. Kazemi, H.A. Rudbari, V. Mirkhani, M. Sahihi, M. Moghadam, S. Tangestaninejad, I. Mohammadpoor-Baltork, Synthesis, characterization, crystal structure, DNA-and HSA-binding studies of a dinuclear Schiff base Zn (II) complex derived from 2-hydroxynaphtaldehyde and 2-picolylamine, J. Mol. Struct. 1096 (2015) 110–120.
[80] M. Mushtaque, M. Jahan, M. Ali, M.S. Khan, M.S. Khan, P. Sahay, A. Kesarwani, Synthesis, characterization, molecular docking, DNA binding, cytotoxicity and

DFT studies of 1-(4-methoxyphenyl)-3-(pyridine-3-ylmethyl) thiourea, J. Mol. Struct. 1122 (2016) 164–174.
[81] N. Shahabadi, S. Mohammadi, R. Alizadeh, DNA interaction studies of a new platinum (II) complex containing different aromatic dinitrogen ligands, Bioinorg. Chem. Appl. 2011 (2011) 8 pages, doi:10.1155/2011/429241.
[82] X. Yang, G.-L. Shen, R.-Q. Yu, Studies on intramolecular charge transfer fluorescence probe and DNA binding characteristics, Microchem. J. 62 (3) (1999) 394–404.
[83] A.H. Wang, Intercalative drug binding to DNA, Curr. Opin. Struct. Biol. 2 (3) (1992) 361–368.
[84] C.A. Frederick, L.D. Williams, G. Ughetto, G.A. Van der Marel, J.H. Van Boom, A. Rich, A.H. Wang, Structural comparison of anticancer drug-DNA complexes: adriamycin and daunomycin, Biochemistry 29 (10) (1990) 2538–2549.
[85] B.H. Geierstanger, D.E. Wemmer, Complexes of the minor groove of DNA, Annu. Rev. Biophys. Biomol. Struct. 24 (1) (1995) 463–493.
[86] S. Takenaka, M. Takagi, Threading intercalators as a new DNA structural probe, Bull. Chem. Soc. Jpn. 72 (3) (1999) 327–337.
[87] G. Bischoff, S. Hoffmann, DNA-binding of drugs used in medicinal therapies, Curr. Med. Chem. 9 (3) (2002) 321–348.
[88] S. Neidle, Crystallographic insights into DNA minor groove recognition by drugs, Biopolymers 44 (1) (1997) 105–121.
[89] S.D. Durgapal, R. Soni, S. Umar, B. Suresh, S.S. Soman, Anticancer activity and DNA binding studies of novel 3, 7-disubstituted benzopyrones, ChemistrySelect 2 (1) (2017) 147–153.
[90] T. Pivetta, E. Valletta, G. Ferino, F. Isaia, A. Pani, S. Vascellari, C. Castellano, F. Demartin, M.G. Cabiddu, E. Cadoni, Novel coumarins and related copper complexes with biological activity: DNA binding, molecular docking and in vitro antiproliferative activity, J. Inorg. Biochem. 177 (2017) 101–109.
[91] W. Ren, Z. Qiao, H. Wang, L. Zhu, L. Zhang, Flavonoids: promising anticancer agents, Med. Res. Rev. 23 (4) (2003) 519–534.
[92] B.P. Bandgar, S.S. Gawande, R.G. Bodade, J.V. Totre, C.N. Khobragade, Synthesis and biological evaluation of simple methoxylated chalcones as anticancer, anti-inflammatory and antioxidant agents, Bioorg. Med. Chem. 18 (3) (2010) 1364–1370.
[93] I. Grigalius, V. Petrikaite, Relationship between antioxidant and anticancer activity of trihydroxyflavones, Molecules 22 (12) (2017) 2169.
[94] F.G. da Silva Dantas, P.F. de Castilho, A.A. de Almeida-Apolonio, R.P. de Araújo, K.M.P. de Oliveira, Mutagenic potential of medicinal plants evaluated by the Ames Salmonella/microsome assay: a systematic review, Mutation Research 786 (2020) 108338.
[95] K. Mortelmans, E. Zeiger, The Ames Salmonella/microsome mutagenicity assay, Mutat. Res./Fundam. Mol. Mech. Mutagen. 455 (1–2) (2000) 29–60.
[96] Ç.K. Karayildirim, M. Kotmakçi, E. Halay, K. Ay, Y. Başpinar, Formulation, characterization, cytotoxicity and Salmonella/microsome mutagenicity (Ames) studies of a novel 5-fluorouracil derivative, Saudi Pharm. J. 26 (3) (2018) 369–374.
[97] J. Serment-Guerrero, M.E. Bravo-Gomez, E. Lara-Rivera, L. Ruiz-Azuara, Genotoxic assessment of the copper chelated compounds Casiopeinas: clues about their mechanisms of action, J. Inorg. Biochem. 166 (2017) 68–75.
[98] S.E. Weinberg, N.S. Chandel, Targeting mitochondria metabolism for cancer therapy, Nat. Chem. Biol. 11 (1) (2015) 9.
[99] M. Kampa, A.-P. Nifli, G. Notas, E. Castanas, Polyphenols and cancer cell growth, Rev. Physiol. Biochem. Pharmacol. 159 (2007) 79–113.
[100] F. Sonmez, Z. Gunesli, B.Z. Kurt, I. Gazioglu, D. Avci, M. Kucukislamoglu, Synthesis, antioxidant activity and SAR study of novel spiro-isatin-based Schiff bases, Mol. Divers. 23 (4) (2019) 829–844.
[101] M. Leopoldini, N. Russo, M. Toscano, The molecular basis of working mechanism of natural polyphenolic antioxidants, Food. Chem. 125 (2) (2011) 288–306.
[102] C.A. Lipinski, Lead-and drug-like compounds: the rule-of-five revolution, Drug Discov. Today 1 (4) (2004) 337–341.
[103] C.A. Lipinski, F. Lombardo, B.W. Dominy, P.J. Feeney, Experimental and computational approaches to estimate solubility and permeability in drug discovery and development settings, Adv. Drug Deliv. Rev. 23 (1–3) (1997) 3–25.
[104] S.A. Hitchcock, L.D. Pennington, Structure– brain exposure relationships, J. Med. Chem. 49 (26) (2006) 7559–7583.
[105] H. Kubinyi, G. Folkers, Molecular Drug Properties: Measurement and Prediction, John Wiley & Sons, 2008.
[106] H. Pajouhesh, G.R. Lenz, Medicinal chemical properties of successful central nervous system drugs, NeuroRx 2 (4) (2005) 541–553.
[107] P.R. Chaturvedi, C.J. Decker, A. Odinecs, Prediction of pharmacokinetic properties using experimental approaches during early drug discovery, Curr. Opin. Chem. Biol. 5 (4) (2001) 452–463.
[108] S. Yee, In vitro permeability across Caco-2 cells (colonic) can predict in vivo (small intestinal) absorption in man—fact or myth, Pharm. Res. 14 (6) (1997) 763–766.
[109] R.D. Brown, M. Hassan, M. Waldman, Tools for designing diverse, druglike, cost-effective, combinatorial library design and evaluation: principles, Softw. Tools Appl. Drug Discov. (2001) 301.
[110] A.K. Ghose, V.N. Viswanadhan, J.J. Wendoloski, A knowledge-based approach in designing combinatorial or medicinal chemistry libraries for drug discovery. 1. A qualitative and quantitative characterization of known drug databases, J. Comb. Chem. 1 (1) (1999) 55–68.